Growth of a SiC layer on Si(100) from adsorbed propene by laser melting

Bogdan Dragnea[a)]
Laboratoire de Photophysique Moléculaire du CNRS, Bâtiment 210 Université de Paris-Sud 91405 Orsay Cedex, France

Jacques Boulmer and Dominique Débarre
Institut d'Electronique Fondamentale, Bâtiment 220 Université de Paris-Sud 91405 Orsay Cedex, France

Bernard Bourguignon[b)]
Laboratoire de Photophysique Moléculaire du CNRS, Bâtiment 210 Université de Paris-Sud 91405 Orsay Cedex, France

(Received 25 September 2000; accepted for publication 17 April 2001)

Carbon is incorporated into Si(100) to form a thin polycrystalline layer of SiC by laser melting the Si surface after adsorption of propene in ultrahigh vacuum. The SiC layer of thickness up to 25 nm is polycrystalline. Crystallites of size ≈100 nm are oriented with respect to the Si substrate and exhibit a diffraction pattern in low energy electron diffraction (LEED). The evolution of the surface is monitored in real time by recording the Si transient reflectivity at 675 nm at each laser pulse, and after exposure to the laser by LEED, IR spectroscopy, and atomic force microscopy. The formation of the SiC layer is accompanied by very strong variations of both the static and transient reflectivities, by the growth and narrowing of the IR peak assigned to β SiC, and by the increase of the C incorporation rate. The SiC overlayer is very stable against photodesorption, while initially small amounts of C on Si are photodesorbed in a few laser pulses. Recording the transient reflectivity during processing allows one to evidence that the laser absorption increases drastically as the SiC layer grows, resulting in (undesired) larger melting depth and duration that favor incorporation of C in Si below the SiC layer. SiC layers of improved quality might be obtained by active control of the laser fluence by means of the reflectivity transient. © *2001 American Institute of Physics.* [DOI: 10.1063/1.1379054]

I. INTRODUCTION

Carbon incorporation in silicon and silicon germanium is of major interest for the realization of silicon based electronic and optoelectronic components based on band gap and strain engineering in IV–IV alloy ($Si_{1-x-y}Ge_xC_y$) heterostructures. Addition of carbon in substitutional sites in Si or SiGe is used mainly to tailor the lattice parameters and the strain in the heterostructures. However, carbon solubility in silicon, at thermal equilibrium, is much lower ($\approx 10^{-5}$) than necessary for this purpose. Actually $Si_{1-x-y}Ge_xC_y$ epilayers with $y \approx 1\%$ may be formed by out of equilibrium growth techniques such as UHV-chemical vapor deposition (CVD),[1] molecular beam epitaxy (MBE),[2] or pulsed laser induced epitaxy (PLIE). In preceding papers, we have shown that PLIE allows the incorporation of C in substitutional sites in Si and $Si_{1-x}Ge_x$ from either C^+ implanted films,[3] or from gas phase using methane and propene.[4] By this method, substitutional C concentrations up to 0.8% have been obtained in $Si_{1-y}C_y$ or $Si_{1-x-y}Ge_xC_y$ films. Larger doses of C result in the growth of silicon carbide (SiC) precipitates, which are quite undesirable in $Si_{1-x-y}Ge_xC_y$/Si heterostructures.[4–6] In fact, these SiC precipitates may be considered as precursors for the growth of a silicon carbide top layer on silicon. In this work, we study the laser induced growth of SiC on Si(100) by PLIE, operated in UHV conditions, C being incorporated from propene adsorbed on the silicon surface.

SiC is a promising material for high power, high temperature, and high frequency microelectronics, provided that reliable and efficient methods can be found to incorporate it in devices. SiC has a large band gap, a high thermal stability, and very good thermal conductivity and electron mobility. However, the deposition of thin layers on top of Si is difficult. The large lattice mismatch of 20% and the differences in thermal expansion between Si and 3C-SiC (or β SiC) results in misfit dislocations and stacking faults.[7] 3C-SiC has been grown on Si by different techniques such as MBE,[8] CVD,[9] supersonic jet epitaxy,[10,11] or laser ablation.[12] Contrary to these techniques which need high substrate temperatures (from 600 to 1400 °C, depending on the technique), SiC growth by PLIE may operate at room temperature. Moreover, the SiC growth is localized to the laser irradiated area, allowing one to realize directly two-dimensional SiC/Si heterostructures on a silicon wafer.

UV laser melting has been known for a long time to allow various types of surface modification, depending on the chemical nature of the adsorbate and/or the gas interacting with Si.[13,14] Several processes are induced and/or strongly enhanced by UV laser melting of Si: desorption, diffusion in the liquid phase, segregation at the solid/liquid interface, and epitaxy from the unmelted solid during cooling. While diffusion in the liquid phase does not vary significantly from one impurity to another, desorption and segregation at the Si liquid/solid interface depend strongly on

[a)]Present address: Dept. of Chemistry, Indiana University at Bloomington, Chemistry Bldg. C125, Bloomington, IN 47405-7102.
[b)]Author to whom correspondence should be addressed; electronic mail: bernard.bourguignon@ppm.u-psud.fr

Downloaded 14 Oct 2007 to 156.56.201.110. Redistribution subject to AIP license or copyright, see http://jap.aip.org/jap/copyright.jsp

the chemical nature of adsorbates. The fraction of adsorbates undersorbed by the laser pulse may be located at the surface or in the bulk, depending on segregation. This has a strong influence on both the final state of the substrate in a single pulse, and on the desorbed fraction at the next pulse. Cleaning, etching, doping, and dopant profile redistribution may occur. Cleaning (in a clean environment, ideally UHV) and etching (in the presence of halogens) are favored by strong desorption and segregation, while doping is favored by small desorption and segregation.

In the literature, the melting dynamics has been measured through time resolved measurements of the Si reflectivity at wavelengths (633 or 675 nm) where solid and liquid Si have very different reflectivities.[15–17] Numerical simulations assume the instantaneous conversion of electronic excitation into heat, and calculate the temperature depth and time profiles as a result of laser absorption and heat flow.[18] They can be compared to transient reflectivity (TR), transient conductance[19] as well as to time unresolved measurements, like impurity depth profile,[20–23] time of flight mass spectrometry,[24] and Auger electron spectroscopy (AES).[24] The competition between desorption and diffusion to the bulk was studied in the case of Cl experimentally[24] and numerically,[25] showing that the branching ratio between desorption and diffusion to the bulk is ''decided'' in the first nanosecond of melting. The surface remains depleted from adsorbates during melting. The influence of impurities at the surface on the melting dynamics has been evidenced recently under conditions of ultrahigh vacuum and single pulse sensitivity, and found to be correlated with changes of the yield of photoemitted conduction electrons.[26] Moreover, numerical analysis of the TR shows that heat diffusion is reduced near the surface during the time of photoexcitation of solid Si.[27] These results suggest that while the melting dynamics is essentially controlled by the temporal profile of the laser pulse and by heat diffusion, the density of conduction electrons is large enough to modify the thermal properties of Si, presumably by weakening the Si–Si bonds.[26,27]

In this work, we report on the formation of a SiC layer on top of Si induced by laser melting under UHV conditions. This is obtained in a few thousand laser pulses at chamber pressures in the range 10^{-8}–10^{-6} mbar. We observe the formation of a SiC layer of thickness up to 25 nm, characterized by a small IR bandwidth of the β SiC vibration and the $c2\times2$ low energy electron diffraction (LEED) pattern of β SiC. The layer is polycrystalline. Crystallites have a size of $\approx$100 nm and they are oriented with respect to the substrate. Monitoring the TR as a function of pulse count allows one to observe strong variations of the melting dynamics during the formation of the SiC layer, which are related to the evolution of the optical and thermal properties as the layer grows. The results show that the pulse energy should be optimized in the course of processing to keep appropriate melting duration and depth.

II. EXPERIMENT

Experiments are carried out under a base pressure of 2×10^{-10} mbar on B-doped 1.5 Ωm Si(100) surfaces. Si cleaning is by heating at 350 °C for 12 h followed by a short anneal to 1100 °C. It is checked by LEED and AES. Sharp LEED patterns are observed before laser processing. The intensity of a s polarized, cw probe laser diode at 675 nm is recorded with a time resolution of 2 ns after its reflection on the silicon sample. The reflected beam is passed through an interference filter and detected by a fast semiconductor detector, the linearity of which is carefully checked. Melting is induced by a pump XeCl laser at 308 nm. The angles of incidence are 0° and 12° for the pump and probe lasers, respectively. The pump beam passes through a lens array homogenizer. The plane where the energy distribution is homogeneous is optically conjugated with the sample, the size of the uniformly irradiated area being $\sim2\times3$ mm^2. The size of the probe laser spot on the sample is 0.1 mm^2. Charges photoemitted by the excimer pulse are collected at 5 mm from the sample on a filament electrode (1 mm diameter, biased +90 V to the sample). At 308 nm only electrons of the conduction band can be photoemitted by absorption of one single photon. The photoelectron current thus reflects the conduction band electron density. The time resolution of $\approx$50 ns does not allow the investigation of the time dependence of photoemission. However, at ''long'' times (>70 ns) a slow signal is observed that corresponds to the laser induced desorption of ions. All signals are recorded on a digital oscilloscope (500 MHz bandwidth) in one single laser shot. Adsorption is made by continuous exposure to propene through a capillary directed towards the sample. The propene pressure in the UHV chamber is tuned in the range 10^{-8}–10^{-6} mbar, but the local pressure is larger by a factor of $\approx$8. This value is estimated by monitoring the evolution of the C incorporation rate as a function of pressure and/or laser repetition rate: saturation of the rate indicates saturation of the surface by propene between two laser shots. Since the sticking coefficient of molecules similar to propene is 1,[28] this allows to calibrate the local pressure. Introduction of propene in the UHV chamber is controlled by means of a quadrupole mass spectrometer. Fourier-transform infrared (FTIR) spectroscopy and atomic force microscopy (AFM) measurements are performed *ex situ*. FTIR absorption spectra are obtained by difference between spectra of laser processed and nonprocessed areas of the sample. The measured integrated absorption peak of β SiC at 798 cm^{-1} is used to derive the thickness of the SiC layer following the calibration of Ref. 29.

III. RESULTS

The shape of the TR as a function of laser fluence is described in detail in Ref. 27. Briefly, the reflectivity of solid Si varies between 0.33 at room temperature and 0.40 at the melting temperature (1683 K), while the reflectivity of liquid Si is 0.7. During melting, the substrate can be described as a multilayered optical system (liquid Si on top of heated layers on top of room temperature Si), and the reflectivity depends on the resulting interference effects. In the case of Si, the reflectivity increases smoothly from 0.33 to 0.70 when the melted depth varies from 0 to $\approx$20 nm with an experimentally observable but small maximum due to the multiple in-

Downloaded 14 Oct 2007 to 156.56.201.110. Redistribution subject to AIP license or copyright, see http://jap.aip.org/jap/copyright.jsp

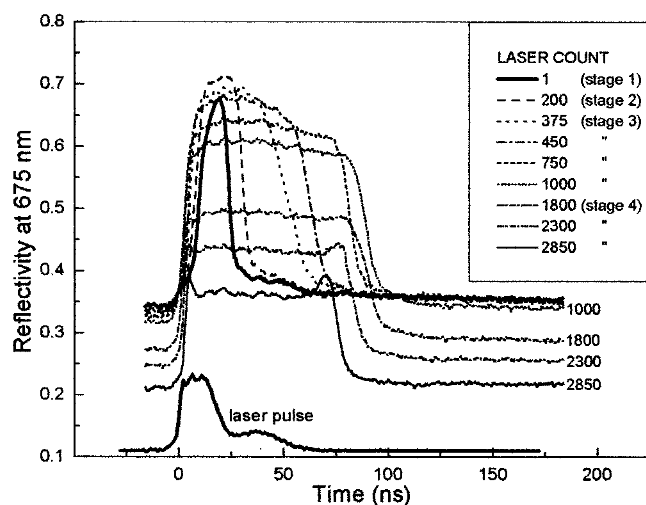

FIG. 1. Evolution with pulse count of the transient reflectivity at 675 nm induced by a laser pulse of 630 mJ cm^{-2} at 308 nm on a Si(100) surface with ≈0.5 ML of propene adsorbed in UHV at each pulse. The transient reflectivity is recorded in a single pulse.

terferences. The TR height R_{max} depends on the melted depth while the width ΔT (measured at $R=0.4$) is the melting duration. Both height and width increase with laser fluence, but the height saturates at the value of liquid Si reflectivity, which is reached when the melted depth equals the liquid Si absorption length at 675 nm (≈20 nm). In this work, the pulse energy is ≈600 mJ/cm^2, resulting on clean Si in a melted depth of ≈17 nm and in a maximum reflectivity R_{max} of ≈0.65. Single-shot TR records of a Si surface with adsorbed propene are shown in Fig. 1. As can be seen in the figure, the formation of the SiC layer on top of Si modifies both the static reflectivity of the solid and R_{max} and ΔT. The evolution of the TR with pulse count shows four successive stages (Table I). The transition from one stage to the next one depends on the parameters that determines the propene dose between two laser shots (i.e., propene pressure and laser repetition rate). In what follows, we indicate the pulse counts (counted from start of growth, not individually for each stage) corresponding to the conditions of Fig. 1, namely a local pressure of 5×10^{-7} mbar and a repetition rate of 1 Hz. Note that the experiments corresponding to Fig. 2 were done at different pressures.

A. Stage 1: Pulses 1–8

The TRs for this stage are not shown in the figures (they can be found in Ref. 26). At the first shot, melting is deeper and lasts longer than on clean Si ($R_{max}=0.67$ and $\Delta T=19$ ns, to be compared to 0.66 and 17 ns). At the next pulses, R_{max} decrease to reach 0.63 at pulse 8. These small changes are attributed in Ref. 26 to variations of the conduction band electron density induced by propene and/or SiC point defects, that affect the thermal properties. On clean Si, the incorporated C dose is calculated to be ≈0.02 ML per pulse, using a numerical simulation of the desorption-diffusion-segregation kinetics (see discussions later). Thus, at this stage the incorporated C dose is <0.16 ML and it is distributed over ≈8 nm (calculated width at half maximum).

B. Stage 2: Pulses 9–≈200

R_{max} and ΔT exhibit large variations, *increasing* up to 0.70 and 30 ns. Assuming that the incorporated dose per laser pulse remains constant with pulse count, this stage corresponds to the transition from a weakly carbonated (<0.16 ML) to a heavily carbonated overlayer (≈4 ML of C distributed near the surface). The FTIR spectrum [Fig. 2(a)] at the end of this stage exhibits essentially a band at the frequency of β SiC (798 cm^{-1}) with a width of 53 cm^{-1}. A peak at ≈600 cm^{-1} corresponding to C in interstitial sites of Si is hardly visible. The integrated peak absorbance corresponds to a thickness of 6 Å, in reasonable agreement with the estimation of 4 ML of incorporated C. In a previous PLIE study at 1.17 J cm^{-2}, C was found only in interstitial sites of Si (band at 600 cm^{-1}) after 100 laser pulses, and mainly (≈94%) in precipitates of β SiC after 300 pulses. Thus, stage 2 corresponds to a transition from substitutional C in Si to SiC. SiC may form either a layer or three-dimensional (3D) islands on top of Si. There is no indication of order of the SiC overlayer by LEED. Only the 2×1 pattern of Si(100) is observed, and it becomes more and more diffuse.

TABLE I. Successive stages of laser induced C incorporation as observed by transient reflectivity.

Stage No.	Number of laser pulses[a]	Melting duration (ns)	C dose at the end of the stage	Chemical nature of C[b]	Static reflectivity
1	1–8	19→17	0.16 ML of C[c]	Interstitial[d]	0.33
2	9–200	17→30	6 Å of β SiC[b]	Interstitial→β SiC	0.33
3	201–1000	30→95	45 Å of β SiC[b]	β SiC+interstitial below SiC	0.33→0.31
4	>1000	95→80	250 Å of β SiC[b,e]	β SiC+interstitial below SiC	0.31→0.20

[a]The number of laser pulses is only indicative: it is valid for a local pressure of 5×10^{-7} mbar at a laser repetition rate of 1 Hz.
[b]From FTIR measurements.
[c]Estimated from numerical simulation of melting and desorption.
[d]From Ref. 4.
[e]For 2850 laser pulses.

Downloaded 14 Oct 2007 to 156.56.201.110. Redistribution subject to AIP license or copyright, see http://jap.aip.org/jap/copyright.jsp

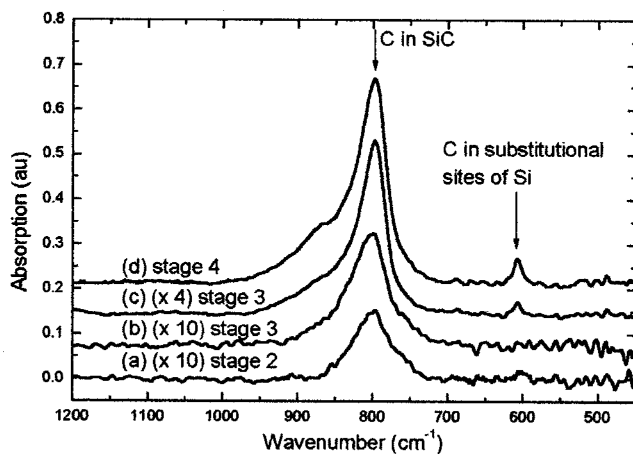

FIG. 2. FTIR absorption spectra of Si processed by PLIE in the presence of propene at 630 mJ cm^{-2} (a) at the end of stage 2, (b) during stage 3, (c) at the end of stage 3, and (d) during stage 4. For clarity, a sensitivity factor is applied to (b), (c), and (d) as indicated on the figure. The local pressure is 2×10^{-5}, 6×10^{-8}, 2×10^{-7}, and 5×10^{-7} mbar, and the number of laser pulses is 400, 4000, 3000, and 2850 for (a)–(d), respectively.

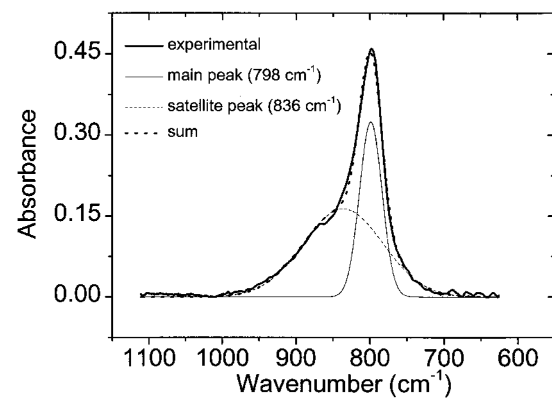

FIG. 3. Deconvolution of the absorption band of Fig. 2(d) corresponding to the stage 4 of SiC layer formation.

C. Stage 3: Pulses ≈200–≈1000

The TR changes dramatically. R_{max} now *decreases* down to 0.60, while ΔT *increases considerably* up to 95 ns (Fig. 1). In addition, the SiC layer becomes thick enough to modify slightly the *static* reflectivity which decreases from 0.33 to 0.31 at pulse 1000. The FTIR absorption spectrum still exhibits mainly the peak of frequency 798 cm^{-1}. However, two other features appear in the spectrum. One is the peak at 607 cm^{-1} corresponding to C atoms occupying interstitial sites in the Si lattice, which (re)appears to reach an intensity of 0.07 relative to the main peak at the transition between stages 3 and 4. The second is a shoulder on the higher frequency side of the peak of β SiC. The deconvolution of the band shows that the amplitude of the shoulder relative to the main peak is rather large (≈0.77). The satellite peak is at 836 cm^{-1}. Its bandwidth is considerably larger (≈3 times) than that of the main peak (which decrease with pulse count down to 42 cm^{-1} at the end of stage 3). The overall intensity of the band (main peak+satellite) corresponds to an SiC thickness of 48 Å at the end of stage 3, showing that the C uptake per laser pulse has significantly increased during stage 3 by a factor of ≈2. If 3D SiC islands were formed initially, it may be expected that they have now coalesced, yielding a better ordered surface. However the LEED pattern at this stage is still a diffuse 2×1.

D. Stage 4: Pulses ≈1000–2850

The static reflectivity changes considerably, going down to 0.20. In addition, R_{max} and ΔT now both decreases (Fig. 1). However, ΔT remains as large as 80 ns (Table I). The FTIR spectrum still exhibits the same features. The band of the Si–C vibration of β SiC at 798 cm^{-1} continues to increase and narrow (down to 36 cm^{-1}). The peak of C at interstitial sites of Si and the shoulder of the β SiC peak keep on increasing faster than the β SiC peak, reaching intensities of 0.11 and 1.8, respectively, after 2850 pulses (Fig. 3). The rate of C uptake (as measured using the integrated FTIR peak intensity of the 8b SiC peak and its shoulder) increase again between stages 3 and 4 by another factor of 2. Since the lattice mismatch between Si and SiC is large, dislocations are expected in the SiC layer. In agreement with this expectation, AFM images of the surface show that SiC is polycrystalline. The size of crystallites is ≈100 nm and the roughness was found in the range 10–20 Å at stages 3 and 4 (Fig. 4). The relationship between roughness and experimental conditions was not systematically studied. However, it seems that the surface is rougher when larger doses of propene are used between laser pulses. In addition, the longer melting at the end of stage 3 seems to result in a rougher surface, the smallest roughness being obtained in the middle of stage 3. Although the SiC layer is polycrystalline, it exhibits at stage 4 the $c(2\times2)$ LEED pattern of β SiC,[30,31] showing that the surface is ordered, and that the crystallites are oriented by the substrate.

IV. DISCUSSION

A. Numerical simulation of the C concentration depth profile on clean Si

We have used a code initially developed for Cl on Si.[25] The C depth profile is calculated as a function of time during

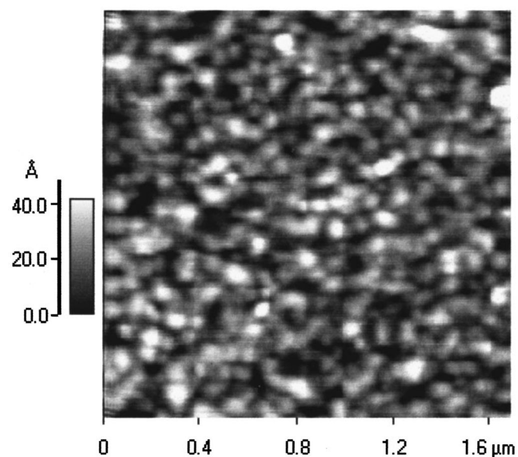

FIG. 4. AFM image of the SiC layer at the beginning of stage 3 [same sample as in Fig. 2(b)]. The measured rms roughness is 9.9 Å.

Downloaded 14 Oct 2007 to 156.56.201.110. Redistribution subject to AIP license or copyright, see http://jap.aip.org/jap/copyright.jsp

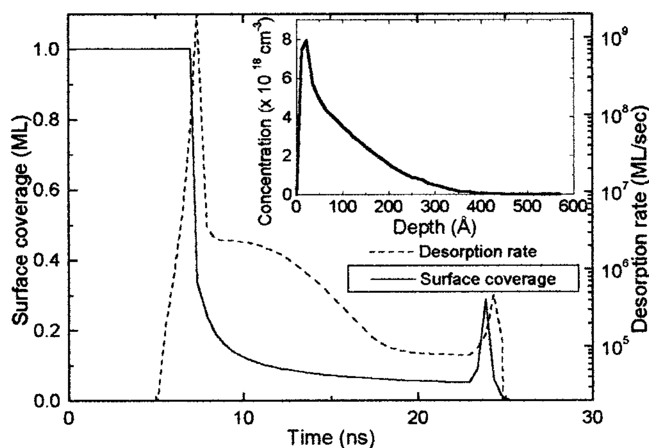

FIG. 5. Calculated propene coverage and desorption rate as a function of time during a laser pulse of 500 mJ cm^{-2}. The laser pulse starts at 0 ns and it has a temporal profile similar to that of Fig. 1. Melting occurs between 7.5 and 24 ns. The inset shows the final C depth profile.

one single laser pulse, taking into account desorption, diffusion in the liquid phase, and segregation at the solid/liquid interface during heating and melting. 1 ML of propene is initially adsorbed on Si. The temporal evolution of the temperature and melted depth are calculated separately, compared with the experimental transient reflectivity, and used as input into the code. The code has been tested with data concerning Cl on Si, which have been fitted to AES results of the Cl remaining on the surface, etch rate measurements, and secondary ion mass spectroscopy depth profile. In the case of Cl, the calculation has shown that the ≈40% fraction of undesorbed Cl spend the time of the laser pulse inside the melted layer, but are found mostly at the surface after the pulse, due to segregation:[24,25] Cl is a case where the final bulk contamination is small, if not negligible. A difference of 0.5 eV was found between the desorption energies from liquid and solid Si, corresponding to the Si latent heat of melting: we assume that it also applies to propene desorption. Propene chemisorbs on Si without dissociation.[28] However, at the high temperature achieved in the present experiments, CH and CC bonds are broken and all H atoms desorb: no signal from CH or CC is observed by FTIR. The unknown desorption energy of propene is assumed to be equal to that of ethylene (1.7 eV),[32] significantly smaller than that of chlorine (3.7 eV). First order desorption with a preexponential factor of 10^{13} s^{-1} is used as for Cl. C experiences a segregation of 0.07 at the liquid/solid interface of Si,[33] to be compared to an upper limit of 0.02 for Cl.[25]

The calculated C concentration depth profile results from the desorption of 98% of the propene ML, 90% being already desorbed when the surface starts melting: propene is a case where bulk contamination is limited by desorption. Figure 5 shows that the surface is depleted very quickly from C, mainly by desorption, but also for a minor part by diffusion into the liquid layer, which results in the presence of C below the surface after melting (shown in the insert). The final C concentration depth profile exhibits a decay with depth (as expected in a case where segregation at the liquid solid interface ''pushes'' C atoms towards the surface during recrystallization). Calculated C depletion in a surface layer of ≈10 Å (insert of Fig. 5) does not fit available experimental depth profiles.[34] It is due to the small desorption energy of propene, which at this stage of the process should be replaced in the calculation by the presumably larger desorption energy of C atoms. This, however, does not influence significantly the time integrated desorbed C, since C desorbs essentially at the very beginning of heating: as can be seen in Fig. 5, the desorption rate falls by ≈3 orders of magnitude after ≈1 ns. The second desorption peak of Fig. 5 appears at the end of melting (after 24 ns) when segregation brings back undersorbed C to the surface. Although this second peak is large enough to influence the final C depth profile, it is very small with respect to the first desorption peak.

B. Laser desorption of propene and C from SiC

The results of the calculation shown in Fig. 5 fit well the incorporation rate of C into Si during stages 1 and 2, as measured by FTIR. However, as the surface evolves into a $c2\times2$ β SiC, the incorporation rate of C increases by a factor of ≈2 between stages 2 and 3, and again ≈2 between stages 3 and 4. Since C incorporation is strongly limited by the desorption of a large fraction of adsorbed propene, this is probably related to a decrease of the desorption rate of propene. Perhaps propene dissociates on SiC, the fragments being more strongly bound than propene, or the desorption energy of propene is simply larger on SiC than on Si. Laser desorption of C is also much stronger on clean Si than on SiC: at stages 1 and 2 the TR returns to that of clean Si in a small number of laser pulses as soon as propene is not readsorbed. Similarly, cleaning of Si from native C (as monitored by AES), is obtained in a few pulses.[24] However, it is no longer the case during stages 3 and 4: laser desorption of the SiC layer is inefficient. The lower desorption rate of propene and its fragments on SiC is also confirmed by the desorbed ion signal induced by the laser at 308 nm, which is observed to decrease by nearly one order of magnitude between stages 1 and 4.

C. Assignment of the FTIR peaks

The bandwidth of vibrational transitions in solids is well known to have homogeneous and inhomogeneous components. The homogeneous part of the bandwidth is due to the finite lifetime of the excited vibrational state, while the inhomogeneous part is due to the fact that the central frequency of a vibrational transition varies with the environment of the vibrator. If vibrators are dispersed in an inhomogeneous medium, the bandwidth may increase beyond the homogeneous width. A value of 28 cm^{-1} was reported for the SiC vibration bandwidth in solid SiC.[35] We find larger values, that are probably related to the inhomogeneous broadening which may be induced in our case by several factors: the distribution of crystallite size, the chemical inhomogeneity in the polycrystalline SiC layer, or even inside crystallites (including the presence of SiC vibrators at the surface of crystallites). It follows that the narrowing of the peak of β SiC during laser processing down to 36 cm^{-1} after 2850 laser pulses most probably suggests that the SiC layer is more and

Downloaded 14 Oct 2007 to 156.56.201.110. Redistribution subject to AIP license or copyright, see http://jap.aip.org/jap/copyright.jsp

more homogeneous as laser processing evolves. However, at the same time, the peak of C at interstitial sites of Si also grows. This may be due to the considerable increase of the melting duration at stages 3 and 4 with respect to stages 1 and 2, and the related larger melted depth: diffusion of C atoms inside Si during melting is easier and easier as the melting duration increases, resulting in a deep, weekly carbonated layer below the SiC layer, where C is most probably at interstitial sites. Clearly, the increase of the melting duration is not desirable and the laser fluence should be lowered at stages 3 and 4, with the expectation of a strong reduction of C diffusion to deep interstitial sites of Si: the FTIR spectrum at the beginning of stage 3 shows that under appropriate conditions the C concentration at interstitial sites may be very small.

The shoulder of the β SiC band might have the same origin. Under the conditions of larger temperature and longer and deeper melting, epitaxy in the liquid phase is expected to occur under a larger heat flow, and more and more out of equilibrium. This is known to reduce segregation and would increase the height and width of the tail of the C depth profile. This may result in the formation of small crystallites of SiC disconnected from the main SiC layer. Such precipitates might be very small, have a broad distribution of size, and be strongly coupled to the Si lattice, which would broaden and presumably shift the Si–C band. Based on the decomposition of the FTIR SiC peaks (Sec. III D and Fig. 3) and assuming a similar vibrational transition probability for SiC in both carbide and substitutional forms, there would be 16 times more carbon in the form of carbide precipitates than in the form of substitutional carbon. As for interstitial C, reducing the laser energy during the PLIE process to keep the melting duration around 20 ns should allow to lower significantly the amounts of this unwanted form of SiC.

D. Variation of the optical parameters during the growth of the SiC layer

The static optical properties of the surface depend on multiple interferences between the reflected beams at the vacuum-SiC and SiC–Si interfaces. The onset of decrease of the static reflectivity at 675 nm at the end of stage 3 implies that both the permanent and transient optical properties change at 308 nm. The permanent change may explain the observed variations of the melting dynamics. Since the thermal and optical parameters of the carbonated layer are not precisely known, we have not attempted the calculation of the melting dynamics. However, we have calculated the static reflectivity of a layer of SiC on Si as a function of SiC thickness at 308 nm (Fig. 6). We used 2.4 and 5×10^3 cm^{-1} for the real and imaginary parts of the refraction index of SiC[36] and the standard values for liquid Si (which are not much different from the solid at 308 nm).[18] SiC and Si differ strongly at 308 nm, SiC absorbing little while Si absorption is very large. As a result, the reflectivity oscillates very strongly as a function of SiC thickness, decreasing from 0.7 to 0.07 at a thickness of $\approx$30 nm. This implies that the laser energy available for melting increases by a factor of $\approx$3 from clean Si to a SiC thickness of $\approx$30 nm. Although this calculation is not accurate, it suggests strongly that the large increase of the melting duration until the end of stage 3, and its decrease during stage 4, are due to optical effects that couple very strongly the SiC/Si system with the laser beam for a certain SiC thickness. As pointed out earlier, this suggests that an active control of the process of SiC growth would be to use the duration of the TR signal to adjust the laser energy at the next laser pulses.

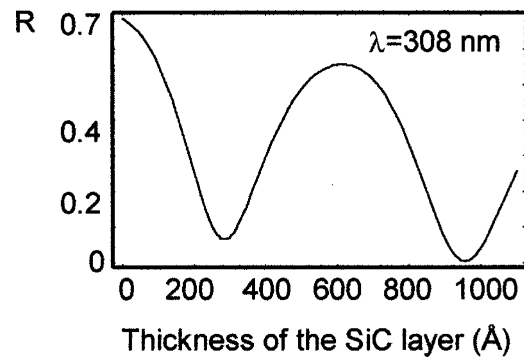

FIG. 6. Calculated reflectivity of a layer of β SiC on top of Si at 308 nm as a function of the SiC thickness.

V. SUMMARY AND CONCLUSION

PLIE is applied to the formation of a SiC layer on Si. A polycrystalline layer of thickness up to 25 nm forms with crystallites of size $\approx$100 nm oriented with respect to the surface and exhibiting a $c2\times2$ LEED pattern. In the conditions used here (i.e., constant laser energy during processing) the SiC crystallites are more and more ordered, but much C is also incorporated beneath the SiC layer, presumably in substitutional sites for Si for a minor part, and in very small SiC precipitates for the main part. TR allows to identify the various stages of the formation of the SiC layer, showing that the melting duration (and presumably depth) increase strongly with SiC thickness. This suggests to use the TR width as an input signal in an active controller of the laser energy. Keeping the melting duration at $\approx$20 ns might allow to improve the quality and usefulness of the SiC layer by minimizing the C concentration below the SiC layer.

ACKNOWLEDGMENT

The authors are very much indebted to Georges Lefèvre for his help on the experiments.

[1] L. T. Vinh, V. Aubry-Fortuna, Y. Zheng, D. Bouchier, C. Guedj, and G. Hincelin, Thin Solid Films **294**, 59 (1997).
[2] K. Eberl, K. Brunner, and W. Winter, Thin Solid Films **294**, 98 (1997).
[3] J. Boulmer *et al.*, J. Cryst. Growth **157**, 436 (1995).
[4] J. Boulmer, C. Guedj, and D. Débarre, Thin Solid Films **294**, 137 (1997).
[5] Z. Kovats, T. H. Metzger, J. Peisl, J. Stangl, M. Muhlberger, Y. Zhuang, F. Schaffler, and G. Bauer, Appl. Phys. Lett. **76**, 3409 (2000).
[6] C. Guedj, M. W. Dashiell, L. Kulik, J. Kolodzey, and A. Hairie, J. Appl. Phys. **84**, 4631 (1998).
[7] L. A. Falkovsky, J. M. Bluet, and J. Camassel, Phys. Rev. B **57**, 11283 (1998).
[8] J. Chen, A. J. Steckl, and M. J. Loboda, J. Vac. Sci. Technol. B **16**, 1305 (1998).

Downloaded 14 Oct 2007 to 156.56.201.110. Redistribution subject to AIP license or copyright, see http://jap.aip.org/jap/copyright.jsp

[9] J. M. Bluet, J. Camassel, L. A. Falkovsky, and A. Leycuras, Diamond Relat. Mater. **6**, 1385 (1997).
[10] Y. Ikoma, T. Endo, F. Watanabe, and T. Motooka, Appl. Phys. Lett. **75**, 3977 (1999).
[11] C. Long, S. A. Ustin, and W. Ho, J. Appl. Phys. **86**, 2509 (1999).
[12] M. Diegel, F. Falk, R. Hergt, H. Hobert, and H. Stafast, Appl. Phys. A: Mater. Sci. Process. **66**, 183 (1998).
[13] D. Bäuerle, *Chemical Processing with Lasers,* Springer Series in Materials Science Vol. 1 (Springer, Berlin, 1986).
[14] I. W. Boyd, *Laser Processing of Thin Films and Microstructures*, Springer Series in Materials Science Vol. 3 (Springer, Berlin, 1987).
[15] G. E. Jellison, Jr. and F. A. Modine, Phys. Rev. B **27**, 7466 (1983).
[16] G. E. Jellison, Jr. and F. A. Modine, J. Appl. Phys. **76**, 3758 (1994).
[17] G. E. Jellison, Jr., D. H. Lowndes, D. N. Mashburn, and R. F. Wood, Phys. Rev. B **34**, 2407 (1986).
[18] S. De Unamuno and E. Fogarassy, Appl. Surf. Sci. **36**, 1 (1989).
[19] P. S. Peercy, M. O. Thompson, and J. Y. Tsao, Appl. Phys. Lett. **47**, 244 (1985).
[20] R. F. Wood and G. E. Giles, Phys. Rev. B **23**, 2923 (1981).
[21] R. F. Wood, J. R. Kirkpatrick, and G. E. Giles, Phys. Rev. B **23**, 5555 (1981).
[22] R. F. Wood, Phys. Rev. B **25**, 2786 (1982).
[23] A. Desmur, B. Bourguignon, J. Boulmer, J.-B. Ozenne, J.-P. Budin, D. Débarre, and A. Aliouchouche, J. Appl. Phys. **76**, 3081 (1994).
[24] B. Bourguignon, M. Stoica, B. Dragnea, S. Carrez, J. Boulmer, J.-P. Budin, D. Débarre, and A. Aliouchouche, Surf. Sci. **338**, 94 (1995).
[25] B. Dragnea, J. Boulmer, J.-P. Budin, D. Débarre, and B. Bourguignon, Phys. Rev. B **55**, 13904 (1997).
[26] B. Dragnea, J. Boulmer, D. Débarre, and B. Bourguignon, Appl. Phys. A (in press).
[27] B. Dragnea and B. Bourguignon, Phys. Rev. Lett. **82**, 3085 (1999).
[28] M. J. Bozack, P. A. Taylor, W. J. Choyke, and J. T. Yates, Jr., Surf. Sci. **177**, L933 (1986).
[29] W. G. Spitzer, D. A. Kleinman, C. J. Frosch, and D. J. Walsh, in *Silicon Carbide: A High Temperature Semiconductor*, edited by J. R. O'Connor and J. Smiltens (Pergamon, New York, 1960), p. 347.
[30] J. M. Powers, A. Wander, P. J. Rous, M. A. van Hove, and G. A. Somorjai, Phys. Rev. B **44**, 11159 (1991).
[31] J. P. Long, V. M. Bermudez, and D. E. Ramaker, Phys. Rev. Lett. **76**, 991 (1996).
[32] L. Clemen, R. M. Wallace, P. A. Taylor, M. J. Dresser, W. J. Choyke, W. H. Weinberg, and J. T. Yates, Jr., Surf. Sci. **268**, 205 (1992).
[33] S. Wolf and R. N. Tauber, *Silicon Processing for the VLSI Era* (Lattice, Sunset Beach, 1992), Vol. 1, p. 251.
[34] R. Tsu, D. Lubben, T. R. Bramblett, and J. E. Greene, J. Vac. Sci. Technol. A **9**, 223 (1991).
[35] Y. H. Seo, K. S. Nahm, E.-K. Suh, and Y. G. Hwang, J. Vac. Sci. Technol. A **15**, 2226 (1997).
[36] H. R. Philipp and E. A. Taft, in *Silicon Carbide: A High Temperature Semiconductor*, edited by J. R. O'Connor and J. Smiltens (Pergamon, New York, 1960), p. 366.

Downloaded 14 Oct 2007 to 156.56.201.110. Redistribution subject to AIP license or copyright, see http://jap.aip.org/jap/copyright.jsp